[Downloaded from www.aece.ro on Thursday, June 12, 2025 at 13:42:19 (UTC) by 172.70.51.247. Redistribution subject to AECE license or copyright.]

Risk-based Optimal Bidding and Operational Scheduling of a Virtual Power Plant Considering Battery Degradation Cost and Emission

Ozge Pinar AKKAS[1], Ertugrul CAM[2]
[1]*Department of Electrical-Electronics Engineering, Kırıkkale University, 71450, Turkey*
[2]*Department of Electrical-Electronics Engineering, Samsun University, 55070, Turkey*
ozgepinarakkas@kku.edu.tr

***Abstract*—A virtual power plant (VPP) is a system combining various types of distributed energy resources (DERs) to provide a reliable power system operation. It provides the advantage of making changes in generation according to variety, price, and demand conditions with bringing renewable energy sources (RES) in a single portfolio and using their flexibility. In this study, it is tried to find optimal bidding and operational scheduling of a VPP containing Wind Power Plant (WPP), Photovoltaic Power Plant (PVPP), Heat-Only Unit (HOU), Battery Energy Storage System (BESS), Combined Heat and Power Plant (CHPP), and electrical/thermal demands and participating in the day-ahead electricity market in 24-h time interval. It is aimed to maximize profit and minimize emissions with considering the battery cost. A stochastic model is formed by considering the uncertainty arising from RES. In addition, CVaR (Conditional Value at Risk) as a risk measurement technique is applied against the risk arising from low profit scenarios. The proposed optimization problem formulated as a stochastic Mixed Integer Nonlinear Programming (MINLP) model and is solved by solver LINDO in GAMS (General Algebraic Modelling System). The case studies are implemented to show the applicability and effectiveness of the presented model.**

***Index Terms*—distributed power generation, energy management, power system planning, renewable energy sources, risk analysis.**

I. INTRODUCTION

The need for energy is increasing exponentially due to the increasing population around the world and technological developments being adapted to daily life rapidly. The energy efficiency and the energy storage are receiving more attention than ever due to increasing electricity demand and targets to be carbon neutral by 2050. The distributed energy generation (DEG) has an important role in improving energy efficiency and generating green energy. The distributed energy resources (DERs) are low capacity and close to the consumer. It reduces losses and transmission cost and improves the power quality. The conventional generators, energy storage systems, microturbines, renewable energy sources (RES) such as wind turbines and photovoltaic panels are among the DERs. The cheap and clean energy is provided by the RES. However, their output power is uncertain since the energy obtained from these sources depends on weather conditions. A Virtual Power Plant (VPP) is an effective solution to the disadvantages of distributed generation systems such as low capacity and uncertain output power. The VPP can combine DERs and controllable loads and participate in electricity markets as a single entity.

There are many studies that deal with optimal operation scheduling of a VPP. Rahimi et al. have presented a VPP model including wind turbines (WTs), conventional generator, photovoltaic modules, energy storage systems (ESS), and controllable loads in the Day Ahead Market (DAM) and Real Time Market (RTM) to maximize profit. They have performed the simulation on a 33-bus distribution network and modeled the problem using GAMS/CPLEX [1]. In another study, Rahimi et al. have proposed a VPP model including WTs, conventional generators, photovoltaic modules, photovoltaic-thermal modules, boilers, ESS, combined heat and power (CHP) to maximize profit [2]. Vahedipour-Dahraie et al. have presented a VPP model consisting of WTs, dispatchable generation units, battery energy storage systems, and flexible loads to maximize profit [3]. In another study, Vahedipour-Dahraie et al. have proposed a model for the VPP bidding strategy in the DAM, RTM and spinning reserve market (SRM) to maximize the profit [4]. Pezhmani et al. have presented a risk-averse decision-making model for the optimal scheduling of a VPP that contains WTs, photovoltaic modules, thermal and electrical storages, heat-only units and heat and power units to maximize its profit [5]. Jafari and Foroud have presented a methodology based on auction theory to form a VPP with considering the risk of energy trading [6]. Yin et al. have presented a novel two-stage robust Stackelberg game for a VPP participating in DAM and RM [7]. Tajeddini et al. have studied on maximizing the VPP operator's expected profit by presenting a two-stage stochastic mixed integer linear programming (MILP). They have used the Value at Risk (VaR) and Conditional Value at Risk (CVaR) risk management models to manage the risks of low profit scenarios and verified that CVaR has a lower profit distribution variance (risk) than VaR [8]. Jordehi has proposed a risk-averse stochastic model for participation of VPP including a CHP unit, WT, battery energy storage (BES), thermal energy storage (TES), heat and electric

This work was supported in part by Kırıkkale University Scientific Research and Projects Coordination Office with the grant number 2018/009.

Digital Object Identifier 10.4316/AECE.2023.02003

1582-7445 © 2023 AECE

[Downloaded from www.aece.ro on Thursday, June 12, 2025 at 13:42:19 (UTC) by 172.70.51.247. Redistribution subject to AECE license or copyright.]

demands with aim the aim of maximizing the expected profit of the VPP and CVaR [9]. However, these studies have not considered the emission in the proposed models. The optimal operation of a VPP with the minimum emission has been crucial due to environmental concerns such as climate change. Therefore, emission criterion should be considered as well as the cost and profit function in the main objective functions.

Heydari et al. have presented a MILP model to maximize the profit of the VPP consisting of DERs, electrical vehicles (EVs) and loads [10]. Yang et al. have presented a bidding model for a VPP with considering different types of EVs integrations [11]. Hadayeghparast et al. have presented a stochastic non-linear model for a VPP to minimize the emission and maximize the profit [12]. Zhang et al. have presented a VPP participating in carbon trading and green certificate trading optimal dispatch model and it is solved by Self-Conclusion and Variational Particle Swarm Optimization (SCV-PSO) algorithm [13]. Akkaş and Çam have presented a VPP model to minimize the emission and maximize the profit with considering the cost of battery degradation [14]. Lamari et al. have proposed a VPP model to reduce operating cost and gas emissions by using a multi-objective feasibility enhanced particle swarm optimization [15]. Wu et al. have presented a VPP model to maximize benefits and minimize carbon emissions with introducing the deep Q network (DQN) in the deep reinforcement learning algorithm [16]. On the other hand, these studies have not considered the risk assessment in the proposed models. It is necessary to control the risk of profit variability and include a suitable risk measure model in the presented problems. Therefore, in this paper, the CVaR that gives a better indication of risk as mentioned in the literature is used as a risk model.

Yang et al. have proposed an optimal bidding strategy model of a VPP aggregating wind farm, photovoltaic panel, gas turbine, energy storage and hydropower station to maximize the whole profit. They studied on the uncertainty modeling for the output of wind farm and photovoltaic panel. However, emission arising from the gas turbine is not taken into account, although its cost function is similar to the conventional thermal power plants. The risk management has not also considered in the study [17]. Wang et al. have proposed a model for a VPP consisting of EVs, distributed generating unit, WTs and ESS. Although distributed generation units such as small gas or diesel units are included in the VPP model, the emission caused by them is not considered in the study. The degradation cost of energy storage is not also considered in the mathematical model [18]. Elgamal et al. have analyzed optimal operation management of a VPP containing solar units, Combined Cooling Heat and Power (CCHP), battery storage system and thermal energy storage system. They have considered the CO_2 emissions born of CCHP, AC and grid power in the model. On the other hand, they have not applied risk control methods in the model and not considered the degradation costs of the storage systems [19]. Sadeghi et al. have proposed an optimal bidding strategy of a VPP including wind generation, distributed generation, energy storage and EVs to maximize the profit. They have considered the emission cost function of distributed generation in the presented model. On the other hand, they have not taken into account the risk management in the VPP bidding strategy and recommended to integrate the operational risk in the future works [20]. Shafiekhani et al. have presented a method for the optimal strategic bidding of a VPP containing wind unit and conventional units. It aims to maximize profit of the VPP and minimize the emission. However, they have not used risk approach in their model [21]. In another study, Shafiekhani et al. have presented a risk-based model for a bidding strategy of a VPP including WTs, traditional units, shiftable and interruptible loads. They have evaluated risk of VPP bidding strategy against load price uncertainty. One of the deficits of this paper is that the emission caused by the traditional units is not considered [22]. Alahyari and Pozo have proposed a VPP model owning wind generation, conventional generation and EVs. They have considered risk management with modeling risk-averse and profit-seeker strategies. However, although conventional generation unit is included in the VPP, the emission has not been covered and the degradation cost of the storage units is not considered in this study [23]. Pandey et al. have presented optimal scheduling of a VPP comprising of RES such as wind power, photovoltaic power and fuel cell among with CHP unit, EV and ESS to maximize the profit and reduce the emission. They have considered CVaR in the risk management model. One of the deficits of this paper is that the ambient temperature and the depth of discharge (DoD), which have a significant effect on the battery life, are not considered in the mathematical expression of the cost of ESS degradation [24].

In the above-mentioned studies, it has been seen that there are some deficits in terms of emission caused by the conventional units, risk evaluation against to the low profit scenarios and degradation cost of the storage units in the optimal operational scheduling and bidding of the VPP. There are few studies that consider both emission and risk evaluation in the proposed model and the deficiencies are also observed in these studies. For example, the degradation cost of the storage systems has not been considered in the proposed model. The batteries used in the storage systems have a cycle life and it is shortened because of deep discharging and high ambient temperature. The degradation cost has important impacts on the optimal scheduling of the VPP decision. In the study of Zhou et al. [25], they have revealed that the expected daily profit of the VPP is reduced by 12.59% with considering the battery degradation cost. They have showed that the DoD and ambient temperature have a significant impact on the degradation cost. Therefore, the DoD and ambient temperature is considered to model the battery degradation cost in this paper.

In this study, a risk-based VPP model attending the Day-Ahead Market (DAM) is proposed. It consists of Wind Power Plant (WPP), Photovoltaic Power Plant (PVPP), Heat-Only Unit (HOU), Battery Energy Storage System (BESS), Combined Heat and Power Plant (CHPP), and electrical and thermal demands. In the proposed model, it is tried to establish an optimal bidding and operation strategy of a VPP that will meet the electrical and thermal demands with maximizing the daily profit of the VPP and minimizing the emission caused by the CHPP, HOU and the power plants in the market. The scenarios are obtained via Scenario

[Downloaded from www.aece.ro on Thursday, June 12, 2025 at 13:42:19 (UTC) by 172.70.51.247. Redistribution subject to AECE license or copyright.]

Reduction and Scenario Tree Construction Algorithms due to the uncertain output powers of WPP and PHPP. For this, the recent past wind and solar data are used. In addition, the battery degradation cost is considered in the objective function. To model the battery degradation cost, the ambient temperature and the DoD, which have a significant effect on the battery life, are considered. Moreover, the CVaR is incorporated into the model to control the risk of encountering low profit scenarios and reduce the profit distribution variance. The presented optimization problem is a Mixed Integer Nonlinear Programming (MINLP), formulated as a stochastic programming model. The problem is solved by LINDO solver that guarantees finding the global optimum solutions to nonlinear problems and finds the appropriate solution in a short time is used to solve the proposed stochastic MINLP problem in GAMS (General Algebraic Modelling System).

II. The Mathematical Model

A. Wind Power Plant Operation Model

The electricity generations from wind energy has increased in the recent years due to its features such as being natural, cost-free, and clean [26]. The available power from the WPP is calculated using (1) for each time and scenario [13], [27].

$$P_{s,t}^{wind}\left(v_{s,t}\right)=N^{wind}\times\begin{cases}0, v_{s,t}<v_i\\ P_{rtd}^{wind}\times\left(\dfrac{v_{s,t}-v_i}{v_{rtd}-v_i}\right)^3, v_i\pounds v_{s,t}\pounds v_{rtd}\\ P_{rtd}^{wind}, v_{rtd}<v_{s,t}\pounds v_o\\ 0, v_o\pounds v_{s,t}\end{cases} \quad (1)$$

where t is index of time periods, s is index of scenarios, N^{wind} is the number of wind turbines in the WPP, $P_{s,t}^{wind}$ indicates the power of the wind turbines at hour t and scenario s (MW), $v_{s,t}$ is the wind speed at hour t and scenario s (m/s), P_{rtd}^{wind} represents the rated power of the wind turbine (MW), v_i is cut-in wind speed, v_{rtd} is rated wind speed, v_o is cut-out wind speed (m/s).

B. Photovoltaic Power Plant Operation Model

A great number of PVPPs have been installed as an alternative to the fossil-fueled power plants in many countries [28]. The available power from the PVPP is calculated using (2)-(6) for each time and scenario [13], [29].

$$T_{s,t}^{C}=T_t^{amb}+SR_{s,t}\times\left(\frac{NOT_C-20}{0.8}\right) \quad (2)$$

$$I_{s,t}=SR_{s,t}\times\left(I_{scc}+K_{ctc}\times\left(T_{s,t}^{C}-25\right)\right) \quad (3)$$

$$V_{s,t}=V_{ocv}-K_{vtc}\times T_{s,t}^{C} \quad (4)$$

$$FF=\frac{V_{Max}\times I_{Max}}{V_{ocv}\times I_{scc}} \quad (5)$$

$$P_{s,t}^{phv}\left(SR_{s,t}\right)=N^{phv}\times FF\times V_{s,t}\times I_{s,t} \quad (6)$$

where $P_{s,t}^{phv}$ represents the power of the solar modules at hour t and scenario s (MW), T_t^{amb} denotes the ambient temperature at hour t (ºC), $T_{s,t}^{C}$ indicates the solar cell temperature at hour t and scenario s (ºC), NOT_C is the nominal operating cell temperature (ºC), $SR_{s,t}$ denotes the solar radiation at hour t and scenario s (kW/m^2), K_{ctc} is the current temperature coefficient of solar module (A/ ºC), I_{scc} is the short circuit current of solar module (A), K_{vtc} is the voltage temperature coefficient of solar module (V/ ºC), V_{ocv} is the open circuit voltage of solar module (V), V_{Max} denotes the voltage at maximum power point of solar module (V), N^{phv} indicates the number of solar modules in the PVPP, FF İs the fill factor of solar module, I_{Max} denotes the current at maximum power point of solar module (A).

C. Combined Heat and Power Plant Operation Model

A concept of Feasible Operation Region (FOR) is used for the CHPP model. FOR is described as the region that the CHPP can generate both heat and electrical power while accepting them as an independent of each other. There are two types of CHP units with convex and non-convex FORs. In this study, the first type of CHP unit with the convex FOR is modeled with (7)-(11) [13], [30].

$$P_t^{com}-P_{com}^{A}-\frac{P_{com}^{A}-P_{com}^{B}}{H_{com}^{A}-H_{com}^{B}}\left(H_t^{com}-H_{com}^{A}\right)\le 0 \quad (7)$$

$$P_t^{com}-P_{com}^{B}-\frac{P_{com}^{B}-P_{com}^{C}}{H_{com}^{B}-H_{com}^{C}}\left(H_t^{com}-H_{com}^{B}\right)\ge\left(1-V_t^{com}\times M\right) \quad (8)$$

$$P_t^{com}-P_{com}^{C}-\frac{P_{com}^{C}-P_{com}^{D}}{H_{com}^{C}-H_{com}^{D}}\left(H_t^{com}-H_{com}^{C}\right)\ge\left(1-V_t^{com}\times M\right) \quad (9)$$

$$0\le P_t^{com}\le P_{com}^{A}\times V_t^{com} \quad (10)$$

$$0\le H_t^{com}\le H_{com}^{B}\times V_t^{com} \quad (11)$$

where P_t^{com} and H_t^{com} are the electrical and thermal output power of the CHPP at hour t, respectively, P^{A}_{com} and P^{C}_{com} are the maximum and minimum operational points of the electrical output power, respectively, H^{B}_{com} and H^{D}_{com} are the maximum and minimum operational points of the thermal output power, respectively, V_t^{com} represents the binary variable that takes the value of '1' or '0' if the CHPP is in 'on' or 'off' status at hour t, respectively, M represents a very large positive number.

The operational cost based on P_t^{com} and H_t^{com} is calculated as shown in (12). The sum of start-up cost, shut-down cost and operational cost gives the total cost of the CHPP as indicated in (13). (14) and (15) state the start-up mode and shut-down mode, respectively.

$$C_t^{com_oc}=a_{com}\times\left(P_t^{com}\right)^2+b_{com}\times P_t^{com}+c_{com}+d_{com}\times\left(H_t^{com}\right)^2+e_{com}\times H_t^{com}+f_{com}\times\left(P_t^{com}\times H_t^{com}\right) \quad (12)$$

$$C_t^{com_tc}=C_t^{com_oc}+C_{start}^{com}\times BU_t^{com}+C_{shut}^{com}\times BD_t^{com} \quad (13)$$

$$BU_t^{com}=V_t^{com}\times\left(1-V_{(t-1)}^{com}\right) \quad (14)$$

$$BD_t^{com}=\left(1-V_{(t-1)}^{com}\right)\times V_t^{com} \quad (15)$$

where $C_t^{com_oc}$ is the operational cost of the CHPP at hour t, $C_t^{com_tc}$ is the total cost of the CHPP at hour t, a_{com}, b_{com}, c_{com}, d_{com}, e_{com}, and f_{com} represent the cost coefficients, C^{com}_{start} and C^{com}_{shut} denote the start-up and shut-down costs,

[Downloaded from www.aece.ro on Thursday, June 12, 2025 at 13:42:19 (UTC) by 172.70.51.247. Redistribution subject to AECE license or copyright.]

respectively, BU_t^{com} and BD_t^{com} represent binary variables indicating the start-up and shut-down modes at hour t, respectively.

D. Heat-Only Unit Operation Model

The heat-only unit is utilized for supplying thermal load. The operational cost of the heat-only unit is given in (16) [13], [31].

$$C_t^{ho} = \alpha_{ho} \times \left(H_t^{ho}\right)^2 + \beta_{ho} \times H_t^{ho} + \gamma_{ho} \quad (16)$$

where C_t^{ho} is the operational cost of the HOU at hour t, α_{ho}, β_{ho}, and γ_{ho} represent the cost coefficients, H_t^{ho} is the thermal output power at hour t.

The constraint of the maximum thermal generation by the HOU is given in (17) [13], [31].

$$0 \le H_t^{ho} \le H_{\max}^{ho} \quad (17)$$

where $H^{ho}{}_{max}$ is the maximum thermal output of this unit.

E. Battery Energy Storage System Operation Model

The BESS is used in the VPP both to meet the shortage of renewable generation and to sell the electricity to the market with high prices. In this paper, lead-acid batteries are used as a storage system. The constraints based on operation of the BESS are given in (18)-(24) [13], [30].

$$0 \le P_t^{ch} \le P_{\max}^{ch} \times s_t^{ch} \quad (18)$$

$$0 \le P_t^{dch} \le P_{\max}^{dch} \times s_t^{dch} \quad (19)$$

$$E_{\min}^{bat} \le SoC_t \le E_{\max}^{bat} \quad (20)$$

$$SoC_{(t=0)} = E_{initial}^{bat} \quad (21)$$

$$SoC_{(t=24)} = E_{final}^{bat} \quad (22)$$

$$s_t^{ch} + s_t^{dch} \le 1 \quad (23)$$

$$SoC_t = SoC_{(t-1)} + \eta_{ch} \times P_t^{ch} - \frac{P_t^{dch}}{\eta_{dch}} \quad (24)$$

where P_t^{ch} and P_t^{dch} are the charging and discharging rate of the BESS at hour t, respectively, P_{ch}^{max} and $P^{dch}{}_{max}$ are the maximum charging and discharging rate, s_t^{ch} and s_t^{dch} indicate the binary variable (1 or 0) if the BESS in charging and discharging modes at hour t, respectively, $E^{bat}{}_{min}$ and $E^{bat}{}_{max}$ are the minimum and maximum energy stored in the storage system, respectively, $E^{bat}{}_{initial}$ and $E^{bat}{}_{final}$ are the initial and final energy level of the storage system, respectively, η_{ch} and η_{dch} represent charging and discharging efficiency of the storage system, respectively, and SoC_t indicates the state of charge (SoC) of the storage system at hour t.

The battery degradation cost can be modeled by the DoD and ambient temperature which have an important effect on the battery cycle life. The DoD for each time is calculated by using (25) [25].

$$DoD_t = 1 - \frac{SoC_t}{E_{bat}^{\max}} \quad (25)$$

The battery cycle life is correlated with the DoD as shown in (26) [25].

$$N_{DoD} = m \times DoD + n \quad (26)$$

where N_{DoD} is the number of cycles stating battery life depending on DoD, m and n indicate cycle life coefficients based on DoD (m=-4230 and n=4332).

The battery cycle life is correlated with ambient temperature as shown in (27) [25].

$$N_{temp} = a \times \exp(bT) \quad (27)$$

where N_{temp} is the number of cycles stating battery life depending on ambient temperature (T (ºC)), a and b indicate cycle life coefficients based on T (a=3291 and b=-0.05922).

The battery cycle life with VPP participation (N_{VPP}) is described with the combination of the effect of T and DoD on battery lifetime as shown in (28) [25].

$$N_{VPP} = \frac{N_{DoD} \times N_{temp}}{N_R} \quad (28)$$

where N_R indicates rated battery cycle life. It can be determined by the manufacturer under rated T and DoD.

The battery degradation cost (F^{BDD}) can be computed with (29) [25].

$$F^{BDD} = \frac{F^{LC}}{N_{VPP} \times E_{total} \times DoD_{ref}} \quad (29)$$

where F^{LC} is the labor cost, DoD_{ref} is the reference DoD, E_{total} indicate the total stored energy in the battery.

F^{BDD} can be obtained for each time with readjusting (29) considering (26)-(28) as shown in (30) [25].

$$F_t^{BDD} = \frac{F^{LC} \times N_R}{\left(m \times DoD + n\right) \times \left(a \times \exp(bT)\right) \times SoC_t \times DoD_{ref}} \times \left(\eta_{ch} \times P_t^{ch} - \frac{P_t^{dch}}{\eta_{dch}}\right) \quad (30)$$

F. Risk Measurement

A risk analysis is carried out in this study to consider the profit volatility risk faced by the VPP participants. The VaR and CVaR are commonly applied risk measure techniques [9], [32]. In this study, the CVaR is used as a risk measurement method due to its advantages over the VaR as mentioned before. The CVaR is stated as the expected value of profit function smaller than (1-α)-quantile of the profit distribution and can be formulated as in (31) [9].

$$CVaR(\alpha, x) = \max\left\{\eta - \frac{1}{1-\alpha} E_w\left\{\max\left\{\eta - f(x,w), 0\right\}\right\}\right\} \quad (31)$$

$\forall \alpha \in (0,1)$

Equations (32)-(34) are used in the risk modeling [9].

$$\eta - \sum_{t=1}^{T}\left[\begin{matrix} MP_t \times P_{s,t}^{mrkt} + RER_t \times P_t^{srv} \\ + HP_t \times H_t^{load} - C_t^{com_tc} - C_t^{ho} - C_t^{BDD} \end{matrix}\right] \le r_s \quad (32)$$

$$Risk = \eta - \frac{1}{1-\alpha} \times \sum_{s=1}^{S} \pi_s \times r_s \quad (33)$$

$$r_s \ge 0 \quad (34)$$

where η and r_s are auxiliary variables used for CVaR calculation and α is the confidence level whose value is in the range (0,1).

G. Objective Functions

The objective functions are to maximize the expected profit and minimize the expected emission in the VPP

[Downloaded from www.aece.ro on Thursday, June 12, 2025 at 13:42:19 (UTC) by 172.70.51.247. Redistribution subject to AECE license or copyright.]

scheduling.

The first objective function (OF1) aims to maximize both profit and risk aversion with considering the risk assessment against low profit scenarios. It is formulated with incorporating the CVaR into the profit maximization model as shown in (35).

$$OF1 = \max(1-\beta)\times\sum_{t=1}^{24}\sum_{s=1}^{S}\pi_s\begin{bmatrix} MP_t\times P_{s,t}^{mrkt}+RER_t\times P_t^{srv} \\ +HP_t\times H_t^{load}-C_t^{com_tc} \\ -C_t^{ho}-F_t^{BDD}\end{bmatrix}+ \quad (35)$$

$$+(\beta\times Risk)$$

where MP_t represents the market electricity price at hour t ($/MWh), π_s denotes the probability of the sth scenario, $P_{s,t}^{mrkt}$ is amount of trading electricity in the market (sold electricity if it is positive, purchased electricity if it is negative), P_t^{srv} is the supplied electricity at hour t, RER_t is the retail price of electricity sale at hour t, HP_t is the price of the heat at hour t, H_t^{load} is the thermal load demand at hour t. The last term (β×Risk) represents the risk measurement. Here, β is the coefficient that indicates the importance of reducing the risk and takes a value between 0-1.

The second objective function (OF2) is to minimize emission and is given in (36). The total expected emission consists of the emissions caused by the power plants in the market, HOU, and CHPP.

$$OF2 = \min\sum_{t=1}^{24} EM_t^{com}+EM_t^{ho}+EM_{s,t}^{mrkt} \quad (36)$$

where $EM_{s,t}^{mrkt}$, EM_t^{ho}, EM_t^{com} are the amount of emission, respectively, caused by the power plants in the market, HOU, and CHPP. They are calculated by (37)-(39), respectively [13]. It is worth to mention that EM_t^{mrkt} is considered in the OF2 if the electricity is bought from the market.

$$EM_t^{com} = \left(NO_x^{com}+SO_2^{com}+CO_2^{com}\right)\times P_t^{com} \quad (37)$$

$$EM_t^{ho} = \left(NO_x^{ho}+SO_2^{ho}+CO_2^{ho}\right)\times H_t^{ho} \quad (38)$$

$$EM_{s,t}^{mrkt} = \left(NO_x^{mrkt}+SO_2^{mrkt}+CO_2^{mrkt}\right)\times\max\left\{-P_{s,t}^{mrkt},0\right\} \quad (39)$$

where NO_x^{com}, SO_2^{com}, CO_2^{com} represent the NO_x, SO_2, and CO_2 emission rates of the CHPP unit, NO_x^{ho}, SO_2^{ho}, CO_2^{ho} represent the NO_x, SO_2, and CO_2 emission rates of the HOU, NO_x^{mrkt}, SO_2^{mrkt}, CO_2^{mrkt} represent the NO_x, SO_2, and CO_2 emission rates of power plants in the market, respectively.

H. Energy Balance Constraints

The electrical and thermal power balance constraints are expressed by (40)-(41).

$$P_{s,t}^{wind}+P_{s,t}^{phv}+P_t^{com}+P_t^{dch}=P_{s,t}^{mrkt}+P_t^{srv}+P_t^{ch} \quad (40)$$

$$H_t^{load}=H_t^{com}+H_t^{ho}-H_t^{sp} \quad (41)$$

The total electrical power generated by WPP, PVPP, CHPP and discharged by BESS must meet the sum of the power sold or purchased to the market (positive if selling, negative if purchasing), the electrical load and the power charged by the BESS as shown in (40).

The total thermal power generated by CHPP and HOU must meet the thermal load. The residual heat power at hour t (H_t^{sp}) is released to the atmosphere.

III. Simulation Studies and Results

A. System Description

In this study, the 380 kV, 22-bus interconnected power system in Turkey in [33] is modified and the proposed VPP model is formed on this power system. The VPP contains a WPP, a PVPP, a HOU, a BESS, a CHPP, and electrical and thermal loads as seen in Fig. 1. In the proposed VPP model, 1 WPP, 1 PVPP, 1 CHPP and 1 BESS are placed on the Bus 17 and this bus is considered as an electrical load bus and the electrical load is met from this bus. The HOU is placed on the Bus 6 that is considered as the thermal load bus and the thermal load is met from this bus. CHPP controls the energy for both busses as it covers both electrical and thermal load.

B. Input Data

The nominal capacity of the WPP containing 3 wind turbines (Enercon E-66) is 5.4 MW. The parameters and values of this turbine are given in Table I [34].

TABLE I. WIND TURBINE PARAMETERS AND VALUES

Turbine type	P_{rtd}^{wind}	N^{wind}	v_i	v_o	v_{rtd}
Enercon E-66	1800 kW	3	2.5 m/s	28 m/s	12 m/s

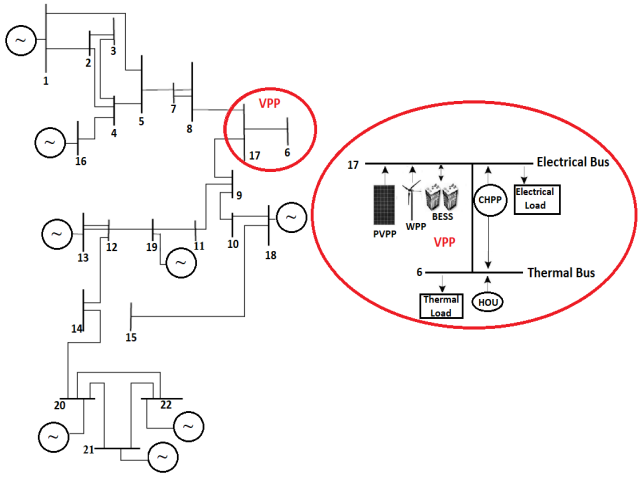

Figure 1. Diagram of the modified 22-bus interconnected system

The nominal capacity of the PVPP containing 50 PV panels is 4.1 MW and the parameters and values of the PV panel are given in Table II [13].

[Downloaded from www.aece.ro on Thursday, June 12, 2025 at 13:42:19 (UTC) by 172.70.51.247. Redistribution subject to AECE license or copyright.]

TABLE II. PV PANEL PARAMETERS AND VALUES

NOT_C	V_{ocv}	V_{max}	I_{max}	I_{scc}	K_{ctc}	K_{vtc}
43 ºC	21.98 V	17. 32 V	4.76 A	5.32 A	0.00122 A/ ºC	0.0144 V/ ºC

The minimum and maximum power values that CHPP can generate are 0.81 MW and 2.47 MW, respectively, and the minimum and maximum heat values that CHPP can generate are 0 MWth and 1.8 MWth, respectively. The parameters and values of the unit in the CHPP are given in Table III [13].

TABLE III. THE UNIT OF CHPP PARAMETERS AND VALUES

Parameters	Value	Parameters	Value
a_{com}	0.0435 ($/MW^2)	e_{com}	0.6 ($/MWth)
b_{com}	56 ($/MW)	f_{com}	0.011 ($/MW.MWth)
c_{com}	12.5 $	C^{com}_{start}	20 $
d_{com}	0.027 ($/MWth^2)	C^{com}_{shut}	20 $

The parameters and values of the unit in the HOU are given in Table IV [13].

TABLE IV. THE UNIT OF HOU PARAMETERS AND VALUES

H^{ho}_{max}	α_{ho}	β_{ho}	γ_{ho}
1.2 MWth	0.052 $/MWth^2	3.0651 $/MWth	4.8 $

The lead-acid batteries are used as ESS. The values of battery parameters in [25] are modified in this paper. The battery parameters and values are given in Table V [14].

TABLE V. THE BATTERY PARAMETERS AND VALUES

Parameters	Value	Parameters	Value
$E^{bat}_{initial}$	0.141 MWh	F^{LC}	$ 152181.5
$E^{bat}_{\min}$	0.141 MWh	N_R	1000
$E^{bat}_{\max}$	1.273 MWh	T	20 □
$P^{\max}_{ch}$	0.283 MWh	η_{ch} , η_{dch}	91.4%
$P^{dch}_{\max}$	0.283 MWh	DoD_{ref}	80 %

The data of electricity, heat and retail price and thermal and electrical load are obtained from [12].

The scenarios have obtained by using the historical data of wind speed and solar radiation through Scenario Reduction and Scenario Tree Construction Algorithms. The hourly wind speed data of the months of March, April and May of 2018 belonging to Çanakkale province are used for wind speed. For solar radiation, hourly solar radiation data of the same months of 2018 belonging to the province of Muğla are used. The profiles of these data are given in Fig. 2. 92 wind speed data are reduced to 10 scenarios via Scenario Reduction and Scenario Tree Construction Algorithms. In the scenario tree, each branch has a probability, and the sum of these probabilities is equal to 1.

The data of wind speed and solar radiation are obtained by reducing to 10 scenarios as shown in Fig. 3.

The probability values corresponding to each scenario are given in Fig. 4.

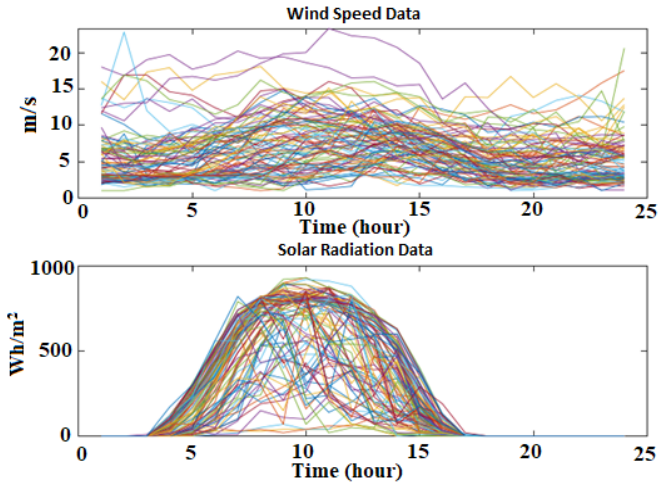

Figure 2. Wind speed and solar radiation data profiles

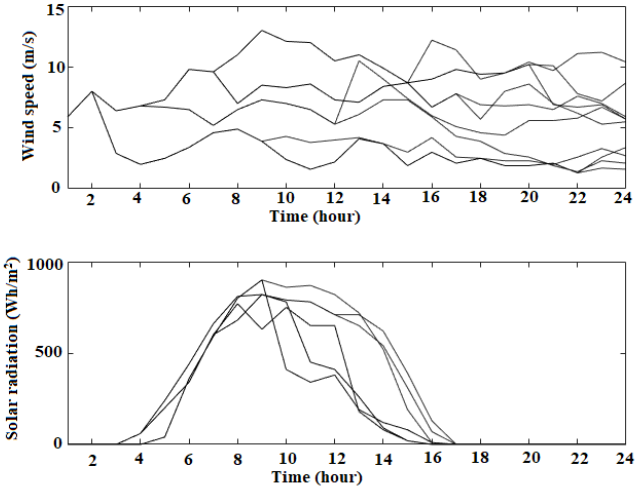

Figure 3. Wind speed and solar radiation values for 10 scenarios

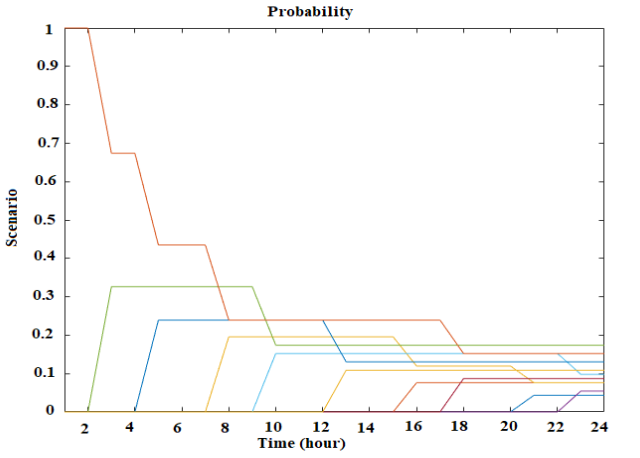

Figure 4. Probability values of scenarios

The risk analysis is also carried out and added to the study. Risk analysis has been done to control the risk of encountering low profit scenarios. For this, CVaR, a risk measurement method, is used. In the problem, the value of α in (33) is taken as 0.90.

C. Results

In this study, three cases are examined. These cases are explained below.

Case 1: Optimum operational scheduling of VPP without considering risk (risk-neutral) (β=0)

[Downloaded from www.aece.ro on Thursday, June 12, 2025 at 13:42:19 (UTC) by 172.70.51.247. Redistribution subject to AECE license or copyright.]

Case 2: Optimum operational scheduling of VPP with equal importance on profit and risk (β=0.5)
Case 3: Optimum operational scheduling of VPP with considering risk (risk-aversion) (β=1)

1) Case 1

In this case, the problem is presented by considering the sources of uncertainty, the cost of battery degradation, minimizing the emission and maximizing the profit. The problem which does not consider the risk is modeled by taking the β value in (35) as 0. The Pareto-based approach is used to find the optimum result and a set of 20 solutions are obtained. The Pareto-optimal solutions are given in Fig. 5.

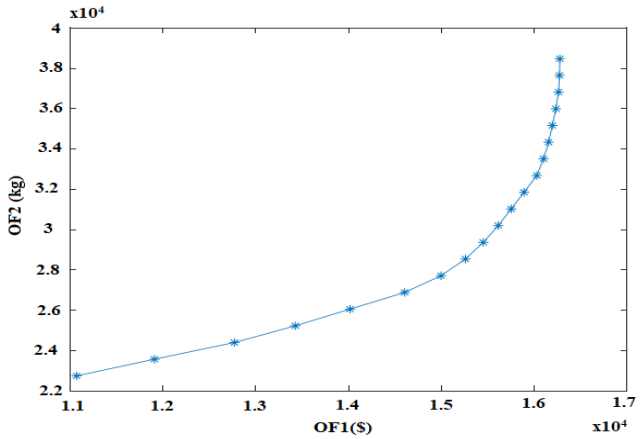

Figure 5. Pareto optimum solutions for Case 1

The optimum solution is chosen among the Pareto optimum solutions for the VPP's operator by using the Fuzzy TOPSIS approach. The VPP's daily profit and amount of emission are obtained as $15894.379 and 31850.161 kg, respectively.

The optimum operational scheduling of the presented VPP for Case 1 is given in Table VI.

TABLE VI. OPTIMUM OPERATIONAL SCHEDULING OF VPP FOR CASE 1

Hours	P_t^{com}	H_t^{com}	H_t^{ho}	P_t^{ch}	P_t^{dch}
1	1.086	1.203	0.381	-	-
2	0.810	1.048	0.536	-	-
3	0.960	1.132	0.452	-	-
4	0.871	1.082	0.502	0.283	-
5	0.810	1.048	0.536	0.283	-
6	0.810	1.048	0.552	0.283	-
7	0.810	1.048	0.424	0.283	-
8	0.810	1.048	0.296	0.107	-
9	2.217	1.424	-	-	-
10	2.361	0.613	0.795	-	0.283
11	2.361	0.613	0.795	-	0.283
12	2.370	0.560	0.768	-	0.197
13	2.208	1.472	-	-	-
14	2.344	0.709	0.843	-	0.118
15	2.194	1.552	-	-	0.037
16	2.194	1.552	-	-	0.030
17	1.708	1.552	-	-	0.016
18	1.848	1.520	-	-	0.015
19	1.245	1.292	0.228	-	0.011
20	1.651	1.520	-	-	0.011
21	2.197	1.536	-	-	0.011
22	0.951	1.127	0.393	-	0.009
23	0.810	1.048	0.456	-	0.008
24	0.810	1.048	0.440	-	0.007

The hourly amount of profit and emission for Case 1 is given in Table VII.

TABLE VII. THE HOURLY AMOUNT OF PROFIT AND EMISSION FOR CASE 1

Hours	Profit ($)	Emission (kg)
1	97.573	939.518
2	146.531	801.883
3	122.031	989.724
4	39.695	1057.777
5	101.288	980.207
6	175.587	808.311
7	228.491	756.888
8	454.682	705.465
9	1307.244	1605.290
10	3044.310	2029.011
11	2784.144	2029.011
12	2184.896	2025.012
13	817.522	1599.111
14	1777.705	2036.208
15	521.747	1588.812
16	493.873	1588.812
17	304.603	1531.898
18	273.935	1657.636
19	282.885	1581.098
20	150.396	1417.255
21	276.789	1589.281
22	116.771	845.850
23	99.212	852.554
24	92.468	833.547

The optimum bidding scheduling of the VPP in the Day Ahead Market for each scenario is given in Fig. 6 for Case 1.

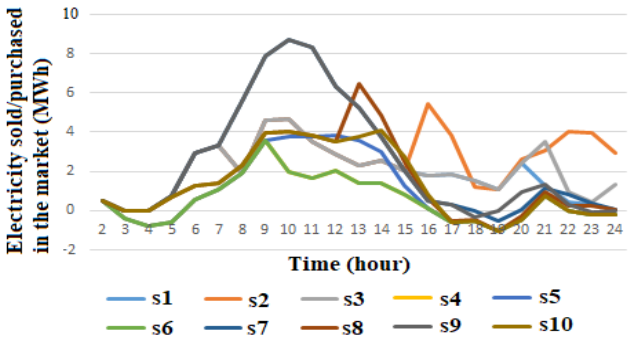

Figure 6. Sold/purchased electricity for 10 scenarios for Case 1

As seen in Fig. 6, it has been observed that electricity is purchased from the market at some times in some scenarios (for example, at 3-5, 17-20, 23-24 hours in scenario 6) because the wind output power is very low at these times. The VPP's operator supplies some of the electricity from the market to meet the electrical load with considering profit and emissions.

2) Case 2

In this case, the problem is presented by considering the sources of uncertainty, the cost of battery degradation, minimizing the emission and maximizing the profit. In the risk analysis, the profit and the risk are equally weighted by taking the β value in (35) as 0.5. The Pareto-based approach is used to find the optimum result and a set of 20 solutions are obtained. The Pareto-optimal solutions are given in Fig. 7.

The optimum solution is chosen among the Pareto optimum solutions for the VPP's operator by using the Fuzzy TOPSIS approach. The VPP's daily profit and amount of emission are obtained as $15856.528 and 31625.101 kg, respectively.

[Downloaded from www.aece.ro on Thursday, June 12, 2025 at 13:42:19 (UTC) by 172.70.51.247. Redistribution subject to AECE license or copyright.]

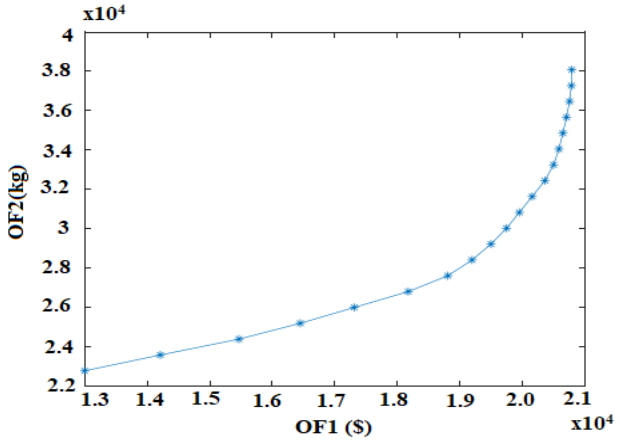

Figure 7. Pareto optimum solutions for Case 2

TABLE VIII. OPTIMUM OPERATIONAL SCHEDULING OF VPP FOR CASE 2

Hour	P_t^{com}	H_t^{com}	H_t^{ho}	P_t^{ch}	P_t^{dch}
1	1.086	1.203	0.381	-	-
2	0.810	1.048	0.536	-	-
3	0.960	1.132	0.452	-	-
4	0.871	1.082	0.502	0.283	-
5	0.810	1.048	0.536	0.283	-
6	0.810	1.048	0.552	0.283	-
7	0.810	1.048	0.424	0.283	-
8	0.810	1.048	0.296	0.107	-
9	2.217	1.424	-	-	-
10	2.342	0.719	0.689	-	0.283
11	2.342	0.719	0.689	-	0.283
12	2.352	0.666	0.662	-	0.197
13	2.208	1.472	-	-	-
14	2.325	0.815	0.737	-	0.118
15	2.194	1.552	-	-	0.037
16	2.194	1.552	-	-	0.030
17	1.708	1.552	-	-	0.016
18	1.848	1.520	-	-	0.015
19	1.245	1.292	0.228	-	0.011
20	1.651	1.520	-	-	0.011
21	2.197	1.536	-	-	0.011
22	0.951	1.127	0.393	-	0.009
23	0.810	1.048	0.456	-	0.008
24	0.810	1.048	0.440	-	0.007

The hourly amount of profit and emission for Case 2 is given in Table IX.

The optimum bidding scheduling of the VPP in the Day Ahead Market for each scenario is given in Fig. 8 for Case 2.

When the results for Case 2 are examined, since β=0.5, the solution that considers profit and risk as equal weight is obtained. It is observed that the amount of profit decreased compared to the amount of profit in Case 1.

3) Case 3

In this case, the problem is presented by considering the sources of uncertainty, the cost of battery degradation, minimizing the emission and maximizing the profit. In the risk analysis, a risk-averse problem is modeled by taking the β value in (35) as 1. The Pareto-based approach is used to find the optimum result and a set of 20 solutions are obtained. The Pareto-optimal solutions are given in Fig. 9.

The optimum solution is chosen among the Pareto optimum solutions for the VPP's operator by using the Fuzzy TOPSIS approach. The VPP's daily profit and amount of emission are obtained as $15812.825 and 31494.645 kg, respectively.

TABLE IX. THE HOURLY AMOUNT OF PROFIT AND EMISSION FOR CASE 2

Hour	Profit ($)	Emission (kg)
1	97.573	939.518
2	146.531	801.883
3	122.031	989.724
4	39.695	1057.777
5	101.288	980.207
6	175.587	808.311
7	228.491	756.888
8	454.682	705.465
9	1307.244	1605.290
10	3044.310	1972.745
11	2744.681	1972.745
12	2175.433	1968.746
13	817.522	1599.111
14	1768.235	1979.942
15	521.736	1588.812
16	493.860	1588.812
17	304.584	1531.892
18	273.913	1657.630
19	282.862	1581.093
20	150.372	1417.252
21	276.815	1589.281
22	116.802	845.860
23	99.245	852.562
24	92.502	833.554

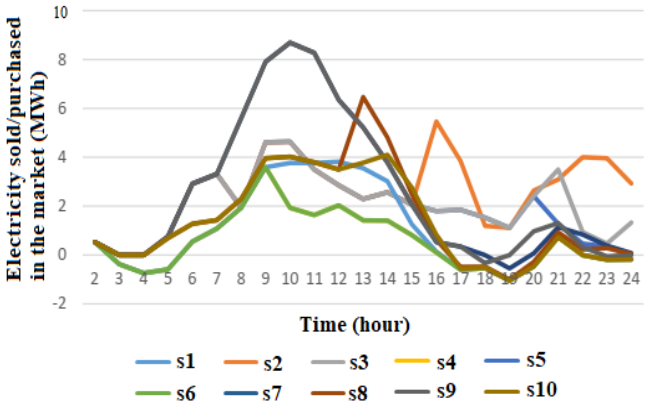

Figure 8. Sold/purchased electricity for 10 scenarios for Case 2

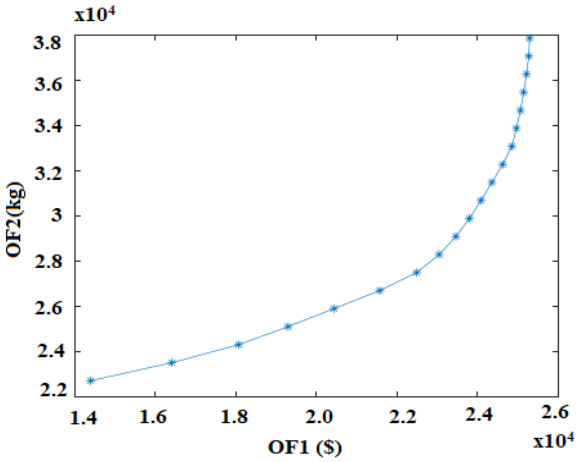

Figure 9. Pareto optimum solutions for Case 3

The optimum operational scheduling of the presented VPP for Case 3 is given in Table X. The hourly amount of profit and emission for Case 3 is given in Table XI.

The optimum bidding scheduling of the VPP in the DAM for each scenario is given in Fig. 10 for Case 3.

When the results in Case 3 are examined, a risk-averse solution is obtained since β=1. The solution is low risk, but the amount of profit has also decreased compared to Case 1 and Case 2.

[Downloaded from www.aece.ro on Thursday, June 12, 2025 at 13:42:19 (UTC) by 172.70.51.247. Redistribution subject to AECE license or copyright.]

TABLE X. OPTIMUM OPERATIONAL SCHEDULING OF VPP FOR CASE 3

Hour	P_t^{com}	H_t^{com}	H_t^{ho}	P_t^{ch}	P_t^{dch}
1	1.086	1.203	0.381	-	-
2	0.810	1.048	0.536	-	-
3	1.243	1.291	0.293	-	-
4	0.810	1.048	0.536	0.283	-
5	0.810	1.048	0.536	0.283	-
6	0.810	1.048	0.552	0.168	-
7	0.810	1.048	0.424	0.283	-
8	0.810	1.048	0.296	-	-
9	2.217	1.424	-	-	-
10	2.325	0.816	0.592	-	0.283
11	2.325	0.816	0.592	-	0.283
12	2.334	0.763	0.565	-	0.197
13	2.208	1.472	-	-	-
14	2.308	0.912	0.640	-	0.118
15	2.194	1.552	-	-	0.037
16	2.194	1.552	-	-	0.030
17	1.708	1.552	-	-	0.016
18	1.848	1.520	-	-	0.015
19	1.245	1.292	0.228	-	0.011
20	1.651	1.520	-	-	0.011
21	2.197	1.536	-	-	0.011
22	0.951	1.127	0.393	-	0.009
23	0.810	1.048	0.456	-	0.008
24	0.810	1.048	0.440	-	0.007

TABLE XI. THE HOURLY AMOUNT OF PROFIT AND EMISSION FOR CASE 3

Hour	Profit ($)	Emission (kg)
1	97.573	939.518
2	146.531	801.883
3	21.027	1130.849
4	98.307	1027.357
5	121.025	945.302
6	178.637	808.311
7	229.999	756.888
8	463.769	705.465
9	1307.244	1605.290
10	3026.174	1921.180
11	2766.007	1921.180
12	2166.759	1917.182
13	817.522	1599.111
14	1759.557	1928.378
15	521.731	1588.812
16	493.853	1588.812
17	304.574	1531.889
18	273.902	1657.626
19	282.850	1581.091
20	150.359	1417.250
21	276.828	1589.281
22	116.817	845.864
23	99.261	852.567
24	92.519	833.558

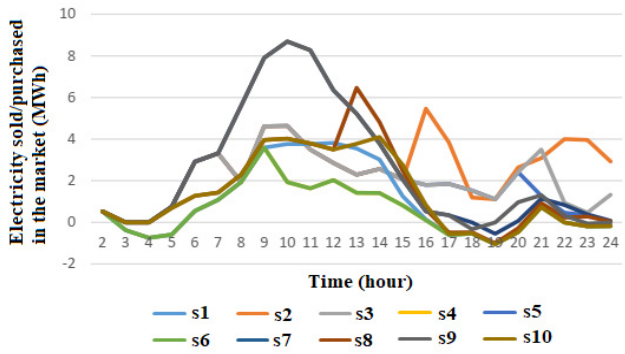

Figure 10. Sold/purchased electricity for 10 scenarios for Case 3

IV. CONCLUSION

In this study, the VPP model formed with the integration of DERs is presented for participation in the DAM and VPP's optimum operational and bidding scheduling is determined hourly to supply both the electrical and thermal demand power and obtain the maximum profit. The gases such as NO_x, SO_2 and CO_2 released from power plants cause global warming by damaging the environment and are one of the most important environmental problems.

Today, the world is in a danger because of climate change. Therefore, the minimization of the released emissions is also considered for VPP's optimum planning. The cost of battery degradation is another important topic addressed in this paper. After a while the battery needs to be replaced since the battery lifetime decreases as it is used. It is an important issue to include the battery degradation cost into the objective function for a more realistic VPP model. Moreover, the uncertainty analysis has been applied with the scenarios based on wind speed and solar radiation historical data due to the uncertainty output power of the WPP and the PVPP through Scenario Reduction and Scenario Tree Construction Algorithms. An appropriate risk measure should be included in the problem to assess the risk of profit variability. The CVaR is a well-known risk measure method and gives a better indication of risk than other methods. Therefore, the risk of low profit scenarios has been evaluated using CVaR. In the simulation study, the proposed stochastic MINLP model is solved using GAMS software. Three cases have been investigated for evaluating the proposed method. In Case 1, a risk-neutral problem model is presented by taking the value of β as 0. The amount of profit and emission are obtained as 15894.379 $ and 31850.161 kg, respectively. In Case 2, a problem model that gives equal importance to both profit and risk is presented by taking the value of β as 0.5. The amount of profit and emission are obtained as 15856.528 $ and 31625.101 kg, respectively. In Case 3, a risk-aversion problem model is presented by taking the value of β as 1. The amount of profit and emission are obtained as 15812.825 $ and 31494.645 kg, respectively. The daily profit of the VPP in case 2 is lower than the profit in the case 1 and the profit in the case 3 is lower than the profit in the case 2. There is a moderate reduction in the expected profit. It shows that CVaR tries to maximize the profit of the lowest profitable scenarios. The VPP operator in Case 1 is risk-neutral and aims to achieve the highest possible profit whatever the risk. The VPP operator in Case 2 prefers a consistent but mean possible profit value. The VPP operator in Case 3 is risk-averse and prefers to keep the minimum profit above a certain amount. The results show that the profit is decreased with the increase in the value of β. However, the risk is also decreases while the profit decreases. Also, it is obtained that there is a decrease in the amount of emissions. Therefore, the model in the Case 2 will be great benefit to VPP participants in the DAM for optimal operational planning and to the VPP's operator for optimal bids.

REFERENCES

[1] M. Rahimi, F. J.Ardakani, O. Olatujoye, and A. J. Ardakani, "Two-stage interval scheduling of virtual power plant in day-ahead and real-time markets considering compressed air energy storage wind turbine," Journal of Energy Storage, vol 45, pp. 103599, January 2022. doi:10.1016/j.est.2021.103599

[2] M. Rahimi, F. J. Ardakani, and A. J. Ardakani, "Optimal stochastic scheduling of electrical and thermal renewable and non-renewable

[Downloaded from www.aece.ro on Thursday, June 12, 2025 at 13:42:19 (UTC) by 172.70.51.247. Redistribution subject to AECE license or copyright.]

resources in virtual power plant," Int J Elec Power, vol. 127, pp. 106658 May 2021. doi:10.1016/j.ijepes.2020.106658

[3] M. Vahedipour-Dahraie, H. Rashidizadeh-Kermani, A. Anvari-Moghaddam, and P. Siano, "Risk-averse probabilistic framework for scheduling of virtual power plants considering demand response and uncertainties," Int J Elec Power, vol. 121, pp. 106126 October 2020. doi:10.1016/j.ijepes.2020.106126

[4] M. Vahedipour-Dahraie, H. Rashidizadeh-Kermani, M. Shafie-Khah, and J. P. S. Catalão, "Risk-Averse Optimal Energy and Reserve Scheduling for Virtual Power Plants Incorporating Demand Response Programs," IEEE T Smart Grid, vol. 12, no. 2, pp. 1405-1415, March 2021. doi:10.1109/TSG.2020.3026971

[5] Y. Pezhmani, M. A. Mirzaei, K. Zare, and B. Mohammadi-Ivatloo, "Robust self-scheduling of a virtual multi-energy plant in thermal and electricity markets in the presence of multi-energy flexible technologies," Int J Energy Res, vol. 46, no. 5, pp. 6225-6245, 2022. doi:10.1002/er.7560

[6] M. Jafari and A. A. Foroud, "A medium/long-term auction-based coalition-forming model for a virtual power plant based on stochastic programming," Electrical Power and Energy Systems, vol. 118, pp. 105784, June 2020. doi:10.1016/j.ijepes.2019.105784

[7] S, Yin, Q. Ai, Z. Li, Y. Zhang, and T. Lu, "Energy management for aggregate prosumers in a virtual power plant: a robust Stackelberg game approach," Int J Electr Power Energy Syst, vol. 117, pp. 105605, May 2020. doi:10.1016/j.ijepes.2019.105605

[8] M. A. Tajeddini, A. Rahimi-Kian, and A. Soroudi, "Risk averse optimal operation of a virtual power plant using two stage stochastic programming," Energ, vol. 73, pp. 958-967, August 2014. doi:10.1016/j.energy.2014.06.110

[9] A. J. Jordehi, "A stochastic model for participation of virtual power plants in futures markets, pool markets and contracts with withdrawal penalty," Journal of Energy Storage, vol. 50, pp. 104304, June 2022. doi:10.1016/j.est.2022.104334

[10] R. Heydari, J. Nikoukar, and M. Gandamkor, "Optimal operation of virtual power plant with considering the demand response and electric vehicles," J Electr Eng Technol, vol. 16, pp. 2407-2419, 2021. doi:10.1007/s42835-021-00784-8

[11] D. Yang, S. He, M. Wang, and H. Pandzic, "Bidding strategy for virtual power plant considering the large-scale integrations of electric vehicles," IEEE Trans Ind Appl, vol. 56, no. 5, pp. 5890-5900, 2020. doi:10.1109/TIA.2020.2993532

[12] S. Hadayeghparast, A. S. Farsangi, and H. Shayanfar, "Day-ahead stochastic multi-objective economic/emission operational scheduling of a large scale virtual power plant," Energy, vol. 172, pp. 630-646, April 2019. doi:10.1016/j.energy.2019.01.143

[13] L. Zhang, D. Liu, G. Cai, L. Lyu, L. H. Koh, and T. Wang, "An optimal dispatch model for virtual power plant that incorporates carbon trading and green certificate trading," Int J Elec Power, vol. 144, pp. 108558, January 2023. doi:10.1016/j.ijepes.2022.108558

[14] Ö. P. Akkaş and E. Çam, "Optimal operational scheduling of a virtual power plant participating in day-ahead market with consideration of emission and battery degradation cost," Int Trans Electr Energ Syst, e12418, 2020. doi:10.1002/2050-7038.12418

[15] M. Lamari, Y. Amrane, M. Boudour, and B. Boussahoua, "Multi□objective economic/emission optimal energy management system for scheduling micro□grid integrated virtual power plant," Energy. Sci. Eng, vol. 10, pp. 3057–3074, 2022. doi:10.1002/ese3.1188

[16] G. Wu, H. Hua, and N. Dongxiao, "Low-carbon economic dispatch optimization of a virtual power plant based on deep reinforcement learning in China's carbon market environment," J Renew Sustain Ener, vol. 14, 056301, 2022. doi:10.1063/5.0107948

[17] C. Yang, X. Du, D. Xu, J. Tang, X. Lin, K. Xie, and W. Li, "Optimal bidding strategy of renewable-based virtual power plant in the day-ahead market," Int J Elec Power, vol. 144, 108557, 2023. doi:10.1016/j.ijepes.2022.108557

[18] J. Wang, C. Guo, C. Yu, and Y. Liang, "Virtual power plant containing electric vehicles scheduling strategies based on deep reinforcement learning," Electr Pow Syst Res, vol. 205, 107714, 2023. doi:10.1016/j.epsr.2021.107714

[19] A. H. Elgamal, M. Vahdati, and M. Shahrestani, "Assessing the economic and energy efficiency for multi-energy virtual power plants in regulated markets: A case study in Egypt," Sustainable Cities and Society, vol. 83, 103968, 2022. doi:10.1016/j.scs.2022.103968

[20] S. Sadeghi, H. Jahangir, B. Vatandoust, M. A. Golkar, A. Ahmadian, and A. Elkamel, "Optimal bidding strategy of a virtual power plant in day-ahead energy and frequency regulation markets: A deep learning-based approach," Int J Elec Power, vol. 127, 106646, 2021. doi:10.1016/j.ijepes.2020.106646

[21] M. Shafiekhani, A. Badri, M. Shafie-khah, and J. P. S. Catalão, "Strategic bidding of virtual power plant in energy markets: A bi-level multiobjective approach," Electrical Power and Energy Systems, vol. 113, pp. 208-219, 2019. doi:10.1016/j.ijepes.2019.05.023

[22] M. Shafiekhani and A. Badri, "A risk-based gaming framework for VPP bidding strategy in a joint energy and regulation market," IJST-T Electr Eng, vol. 43, pp. 545-558, 2019. doi:10.1007/s40998-019-00179-6

[23] A. Alahyari and D. Pozo, "Performance-based virtual power plant offering strategy incorporating hybrid uncertainty modeling and risk viewpoint," Electr Pow Syst Res, vol. 203, 107632, 2022. doi:10.1016/j.epsr.2021.107632

[24] A. K. Pandey, V. K. Jadoun, and N. S. Jayalakshmi, "Real-time and day-ahead risk averse multi-objective operational scheduling of virtual power plant using modified Harris Hawk's optimization," Electr Pow Syst Res, vol. 220, 109285, 2023. doi:10.1016/j.epsr.2023.109285

[25] B. Zhou, X. Liu, Y. Cao, C. Li, C. Y. Chung, and K. W. Chan, "Optimal scheduling of virtual power plant with battery degradation cost," IET Gener Transm Dis, vol. 10, no. 3, pp. 712-725, 2016. doi:10.1049/iet-gtd.2015.0103

[26] T. Depci, M. İnci, M. M. Savrun, and M. Büyük, "A review on wind power forecasting regarding impacts on the system operation, Technical Challenges, and Applications," Energy Technology, vol. 10, no. 8, 2101061, 2022. doi:10.1002/ente.202101061

[27] S. Nojavan, K. Zare, and B. Mohammadi-Ivaltloo, "Application of fuel cell and electrolyzer as hydrogen energy storage system in energy management of electricity energy retailer in the presence of the renewable energy sources and plug-in electric vehicles," Energy Conversion and Management, vol. 136, pp. 404-417, March 2017. doi:10.1016/j.enconman.2017.01.017

[28] V. Thakur and S. S. Chandel, "Maximizing the Solar Gain of a Grid-Interactive Solar Photovoltaic Power Plant," Energy Technology, vol. 1, no. 11, pp. 661-667, 2013. doi: 10.1002/ente.201300118

[29] A. G. Zamani, A. Zakariazadeh, and S. Jadid, "Stochastic operational scheduling of distributed energy resources in a large scale virtual power plant," International Journal of Electrical Power & Energy, vol. 82, pp. 608-620, November 2016. doi:10.1016/j.ijepes.2016.04.024

[30] M. Nazari-Heris, S. Abapour, and B. Mohammadi-Ivatloo, "Optimal economic dispatch of FC-CHP based heat and power micro-grids," Applied Thermal Engineering, vol. 114, pp. 756-769, March 2017. doi:10.1016/j.applthermaleng.2016.12.016

[31] M. Nazari-Heris, M. Mehdinejad, B. Mohammadi-Ivatloo, and G. Babamalek-Gharehpetian, "Combined heat and power economic dispatch problem solution by implementation of whale optimization method," Neural Computing and Applications, vol. 31, no. 2, pp. 421-436, 2019. doi:10.1007/s00521-017-3074-9

[32] A. Castillo, J. Flicker, C. W. Hansen, J-P. Watson, and J. Johnson, "Stochastic optimisation with risk aversion for virtual power plant operations: a rolling horizon control," IET Gener Transm Dis, vol. 13, no. 11, pp. 2063-2076, 2019. doi:10.1049/iet-gtd.2018.5834

[33] U. B. Filik and M. Kurban, "Optimal power flow analysis of the 22-bus 380-kV interconnected power system in Turkey," IEEE International Power and Energy Conference, pp. 276-279, 2006. doi:10.1109/PECON.2006.346662

[34] B. Ozerdem, S. Ozer, and M. Tosun, "Feasibility study of wind farms: A case study for Izmir, Turkey," J Wind Eng Ind Aerod, vol. 94, no. 10, pp. 725-743, October 2006. doi:10.1016/j.jweia.2006.02.004